Journal of Applied Geodesy 1 (2007), 137–145 © de Gruyter 2007. DOI 10.1515/JAG.2007.016

Monitoring of the reflectors of ESA's Planck telescope by close-range photogrammetry

Jafar Amiri Parian, Armin Gruen, Alessandro Cozzani

Abstract. The Planck mission of the European Space Agency (ESA) is designed to image the anisotropies of the Cosmic Background Radiation Field over the whole sky. Planck's objective is to analyze, with the highest accuracy ever achieved, the remnants of the radiation that filled the universe immediately after the Big Bang, which we observe today as the cosmic microwave background. To achieve this aim well-manufactured reflectors are used as parts of the Planck telescope receiving system. The system consists of the Secondary and Primary Reflectors which are sections of two different ellipsoids of revolution with diameters of 1.1 and 1.9 meters. Deformations of the reflectors which influence the optical parameters and the gain of receiving signals are investigated in vacuum and at temperatures down to 95K, using close-range photogrammetric techniques. We have designed an optimal close-range photogrammetric network by heuristic simulation for the Primary and Secondary Reflectors with a mean relative precision better than 1 : 1,000,000 and 1 : 400,000, respectively, to achieve the requested accuracies. Special considerations have been taken into account in different steps of design, such as the determinability of additional parameters under the given network configuration, datum definition, reliability and precision issues as well as workspace limits and propagating errors from different sources of errors. A least squares best-fit ellipsoid was developed to determine the optical parameters of the reflector. We present our procedure and the results of processing the photogrammetric measurements of the Flight Models of the Primary and Secondary Reflectors which were executed by Thales Alenia Space France under ESA-ESTEC contract in vacuum and at very low temperatures.

Keywords. Planck telescope, photogrammetric network design, system calibration, deformation monitoring, best-fit ellipsoid.

1. Introduction

The Planck mission of ESA, which is planned for launch in 2008 will collect and characterize radiation from the cosmic microwave background using sensitive radio receivers operating at extremely low temperatures. Planck's objective is to analyze, with the highest accuracy ever achieved, the remnants of the radiation that filled the universe immediately after the Big Bang, which we observe today as the Cosmic Microwave Background (CMB). Planck was selected as the third Medium-Sized Mission (M3) of ESA's Horizon 2000 scientific program, and is today part of its Cosmic Vision program. It is designed to image the anisotropies of the cosmic background radiation field over the whole sky, with unprecedented sensitivity and angular resolution. Planck will help to provide answers to one of the most important sets of questions asked in modern science – how did the universe emerge, how did it evolve to the state we observe today, and how will it continue to develop in the future? The Planck mission will collect and characterize radiation from the CMB using sensitive radio receivers. These receivers will determine the black body equivalent temperature of the background radiation and will be capable of distinguishing temperature variations of about one micro-Kelvin. These measurements will be used to produce the best ever produced maps of anisotropies in the CMB radiation field (Tauber 2000, Passvogel and Juillet 2003).

To achieve this aim well-manufactured reflectors are used as part of the Planck telescope receiving system (Figure 1). The telescope consists of the Secondary Reflector (SR) and the Primary Reflector (PR) which are specific sections of two different ellipsoids of revolution with diameters of 1.1 m and 1.9 m (Table 1). Deformations of the reflectors which influence the optical parameters and the gain of the received signals need to be measured in vacuum and at temperatures down to 95K. This is required to investigate the correlation of the thermo-elastic model used for the reflector design with the actual performance. Surface accuracy and optical parameters (radius of curvature and conic constant) and their precisions are requested parameters defined by the European Space Technology and Research Center of ESA (ESA-ESTEC).

Figure 2 shows the workflow of the project. The performed tasks are divided into two groups: network design and real measurements. The scope of the first group is the close-range photogrammetric network design and associated procedures for the PR and SR. The scope of the second group is the real measurements of the Primary Reflector Flight Model (PRFM) and Secondary Reflector Flight Model (SRFM).

Beside of high accuracy measurement techniques, like Coordinate Measurement Machine (CMM) and interferometery, photogrammetric technique was used in practice due to its efficiency that can more conveniently be applied for cryo-temperature measurements. For the deformation monitoring of the reflectors the concept of hyper-image digital photogrammetry was

Figure 1: Planck Telescope (left). The telescope structure (right) with primary reflector (top) and secondary reflector (bottom). Copyright ESA, right view courtesy Thales Alenia Space France.

Table 1: Specifications of the Primary and Secondary Reflectors.

Parameters	Primary Reflector	Secondary Reflector
R (radius of curvature) (mm)	*1440.000*	*−643.972*
K (conic constant)	*−0.86940*	*−0.215424*
Elliptical contours (mm × mm)	*1555.98 × 1886.79*	*1050.96 × 1104.39*

used in design and practice. This is based on extremely high network redundancy and the modeling of possible systematic errors. Based on the designed photogrammetric network real tests were executed by Thales Alenia Space France (TASF) under ESA-ESTEC contract.

We present our procedure, including different steps of design and the results of real measurements of the PRFM and SRFM, which indicates a mean relative precision better than 1 : 1,000,000 and 1 : 400,000, respectively.

Performed task	Scope of the task	Details of the task
Network design	PR and SR	– Developing best-fit ellipsoid – Second Order Design: Std. dev.(R, K) → std. dev. (X,Y,Z) – Zero Order Design: Best datum selection – First Order Design: Close-range photogrammetric network design by heuristic simulation
	⇩	
Real measurements	PRFM and SRFM	– Bundle block adjustment & self-calibration – Best-fit ellipsoid

Figure 2: Workflow of the project. It consists of mainly two steps: Network design and real measurements.

2. Network design

The purpose of the network design is to design an optimum network configuration and an optimum observation plan that will satisfy the pre-set quality requirements with a minimum of effort. For the sake of simplicity, the design problem was divided into three sub-problems according to the concept of network design, which was proposed by Grafarend 1974. The design steps were applied in the following order:

1) Second Order Design (SOD)
   To relate 3D point coordinates with optical parameters of the reflector, a best-fit ellipsoid was developed and based on it, SOD was performed to determine the required precision of the point coordinates with respect to the precision of the requested optical parameters.
2) Zero Order Design (ZOD)
   To choose a suitable datum in order to achieve the best possible precision for the optical parameters.
3) First Order Design (FOD)
   A close-range photogrammetric network was designed by heuristic simulation in order to obtain the precision of the point coordinates which matches the estimated precision of the first step (SOD).

2.1. *Best-fit ellipsoid and Second Order Design (SOD)*

The SR is a section of an ellipsoid of revolution around a Z-axis with a and b as principal axes (equation (1)).

$$\frac{X^2}{b^2}+\frac{Y^2}{b^2}+\frac{Z^2}{a^2}=1 \tag{1}$$

The optical parameters, (K and R), of the reflector are computed by equations (2)–(3):

$$K=E^2, \quad \text{with } E=\sqrt{1-\frac{b^2}{a^2}} \tag{2}$$

$$R=a(1-E^2) \tag{3}$$

in which K, R and E are the conic constant, the radius of curvature and the eccentricity, respectively.

Equation (1) is a standard form of an ellipsoid of revolution with aligned principal axes to the axes of the coordinate system and the ellipsoid center at the origin. In the case of a different coordinate system of the point cloud with respect to the coordinate system of the axes aligned ellipsoid, an appropriate transformation is used for mapping the point cloud to the ellipsoid coordinate system. Our solution for determination of optical parameters is a best-fit ellipsoid based on least squares minimization of the distances of the point cloud from the ellipsoid.

The requested accuracies are related to the optical parameters of the reflector which were defined by ESA-ESTEC. These parameters cannot be measured directly with photogrammetry. Therefore points on the surface of the reflector are measured and the optical parameters are estimated using the developed best-fit ellipsoid method. These points in our case are the centers of circular retro-reflective targets.

The distribution of targets, the number and precision of the point coordinates are the factors that influence the precision of the optical parameters. Since the reflector is a section of an ellipsoid, it has different curvatures in different areas. Therefore the targets have to be distributed such that there exist a sufficient number in areas of higher curvature. In addition, the increase of the number of points improves the precision of the optical parameters. Another important factor is the precision of the point coordinates.

Since the configuration is known, the problem in this step is to decide about the weights of the observations (point coordinates) to meet the design criteria. The precision values of the observations are estimated by SOD. In other words, the weight matrix of observations, which are X, Y and Z coordinates, are estimated from the covariance matrix of unknowns, which are the optical parameters. For very strong geometrical networks with a relatively large number of targets, it can be assumed that this weight matrix is approximately a diagonal matrix. The solution of SOD is selected based on the method which estimates the diagonal of the weight matrix. It is an iterative method proposed by Wimmer (1982) and is a direct approximation of the weight matrix based on Q_{XX} (cofactor matrix of target center coordinates).

However, to be sure that the diagonal weight matrix, which is constructed by the estimated precision of the point coordinates from SOD is fulfilling the requirements, error propagation was done to estimate the precision of the optical parameters. In addition, the target thickness and the uncertainty of target thickness were modeled in the best-fit ellipsoid for the error propagation.

Considering the potential accuracy of the photogrammetric method and the possible number of targets that could be stuck on the surface of the PR and the SR, successful results were achieved by using approximately 1000 and 450 targets that were distributed homogeneously on the surface of the reflectors. Contrary to our optimal design concept of adjusting the target density to the local curvature, we used here a homogeneous distribution because in this case sticking was easier and at the same time we did get a sufficient density in all curvature areas.

2.2. *Datum definition or ZOD*

For an accurate estimation of the optical parameters appropriate datums were selected. Two datum choices were used for the estimation of these parameters:

– an inner constraints datum for resolving a datum defect of rank 7
– with a known distance, an inner constraints datum for resolving the remaining 6 datum parameters.

An inner constraints datum for resolving 7 datum parameters is the best datum for the estimation of the conic constant because this parameter is scale-independent. The first datum cannot be used for the estimation of radius of curvature because this parameter is scale-dependent. The scale is defined by a scale-bar with a known distance and its uncertainty.

2.3. *Close-range photogrammetric network design by heuristic simulation or FOD*

Previous research on this topic in close-range photogrammetry was done by Fraser (1984, 1992, 1996) who discussed the network design problems in close-range photogrammetry. Fritsch and Crosilla (1990) performed first order design with an analytical method. Mason (1994) used expert systems and Olague (2002) used a genetic algorithm for the placement of matrix array cameras using heuristic computer simulation. Visibility analysis by a fuzzy inference system for the camera placement was done by Saadatseresht et al. (2004). Precision and reliability considerations in close-range photogrammetry, as a part of the network quality requirements, have been addressed by Gruen (1978, 1980) and Torlegard (1980). Considerations on camera placement for the determination of the additional parameters of the camera by using control points were addressed by Gruen and Beyer (2001). The relation between highly redundant image acquisition and the related very high accuracy in point coordinates was already demonstrated by Amiri Parian (2004) and Fraser et al. (2005).

The aim of heuristic simulation is to design an optimal close-range photogrammetric network with a precision which matches the required values from the previous step, SOD. In addition to the work space limits and the existing facilities for the placement and orientation of the camera, the network should also be able to:

– de-correlate (at least partially) the point coordinates with respect to the other parameters (the exterior orientation and additional parameters of the camera),
– estimate additional parameters reliably,
– reduce the influence of the variation in reflectivity of the retro-reflective targets,
– reduce the error of image target center (eccentricity) by selecting an appropriate location and orientation of the camera and a suitable target size. The image target center error is the error of the measured target center with respect to the physical target center because of the perspective projection effect.

Considering the existing facilities of TASF (with the capability to operate at low temperatures) a network was designed that satisfies the above 4 conditions. Figure 3 and Figure 4 show the configuration of the camera stations with respect to the PR and the SR. The network consists of 70 stations with 1 image per station. The incidence angle of the camera optical axis with respect to the aperture of the PR is 30 degrees and with respect to the aperture of SR, 45 degrees. With the assumption, based on our previous measurement experience (Amiri Parian et al. 2006), that the internal accuracy of the camera system is 1/70 of a pixel, the mean relative precisions of the networks are better than 1 : 1,000,000 and 1 : 400,000 for PR and SR respectively.

3. Results of real measurements

Previous measurements of the Planck reflectors were related to the Qualification Model of SR (SRQM) (Amiri Parian et al. 2006) which were performed in vacuum, at temperatures down to 95 K and at 13 epochs. In the measurement of SRQM, most of the targets fell off and were unstable during image acquisition because of loss of target adhesion at low temperatures. From the experience of that measurement, suitable adhesion and type of targets were selected for the measurements of the Flight Models of the Primary and Secondary Reflectors.

The Flight Model of the Primary Reflector (PRFM) and Secondary Reflector (SRFM) were measured independently by TASF under ESA-ESTEC contract according to the designed network. The measurements were done in vacuum and at temperatures down to 95K, in total at 11 epochs using a 6-MegaPixel commercial frame array CCD camera. Approximately 2400 and 1200 targets were stuck homogeneously on the surface of the PRFM and SRFM. Here the number of targets was increased compared to the number of targets in the simulation. The monitoring of the small scale features of the reflectors and the availability of sufficient number of targets at low temperatures in the case of target fall-off were the reasons of sticking more targets than the estimated number in the design step.

Due to a high demand for a quick feedback to ESA-ESTEC and TASF concerning the approval of a successful measurement at each epoch, a rapid computation was performed through Limiting Error Propagation (LEP) method (Fraser 1987) only for the computation of the standard deviations of the object point coordinates. LEP was applied successfully because of very strong network geometry and the large amount of targets. However, to investigate the relation of the Total Error Propagation (TEP) to the LEP in this network configuration, groups of re-sampled object points with 300, 450 and 600 targets were selected and bundle adjustments were run with the TEP and the LEP methods. The standard devia-

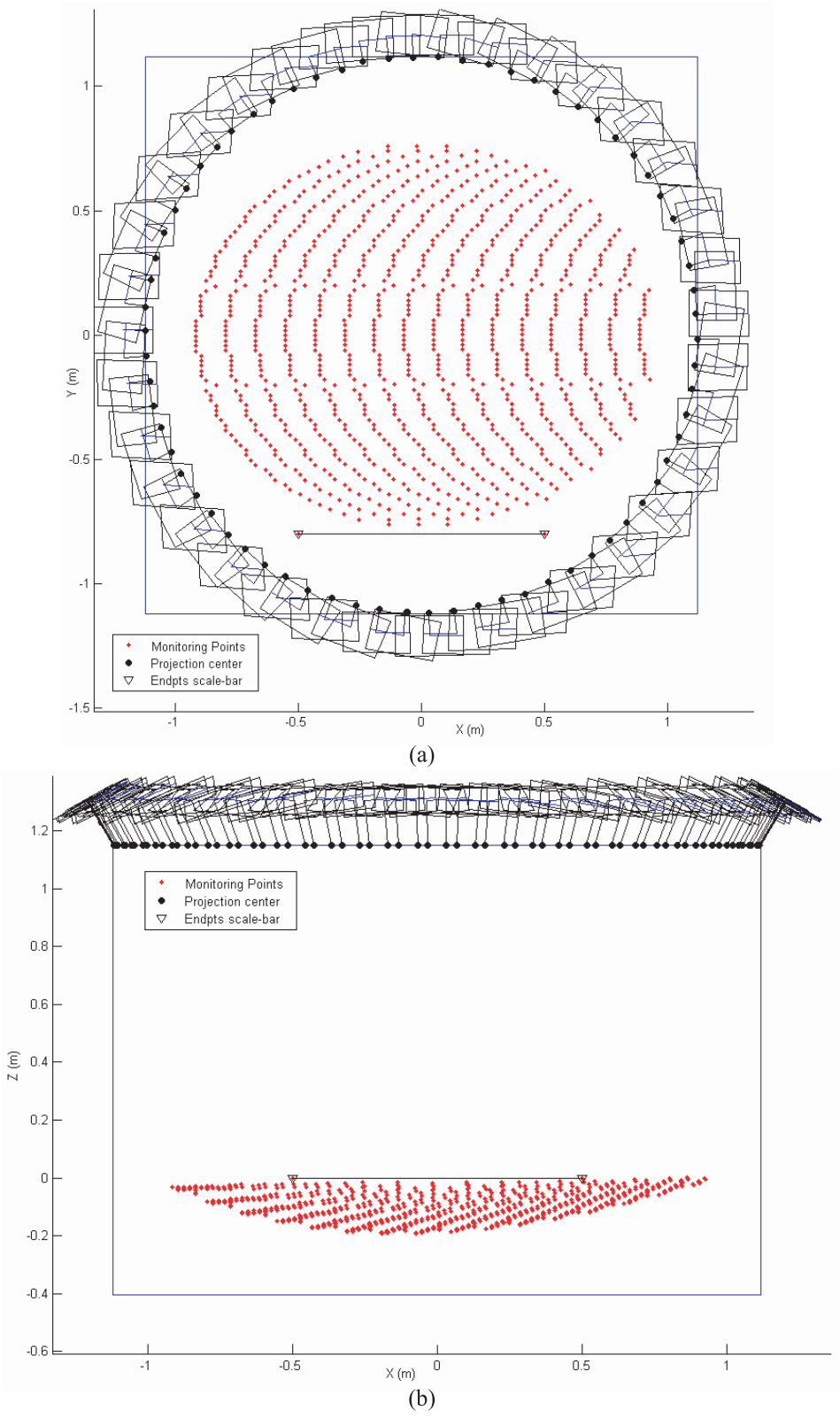

Figure 3: Network configuration for PR. (a) XY-view and scale-bar, (b) XZ-view of the network.

tions from the LEP of these versions were better than the standard deviations from TEP by a factor of maximal 1.2. This factor was used to convert the final LEP standard deviations to TEP standard deviations.

The mean relative precision values of the real networks are in good agreement with the simulated networks and are better than 1 : 1,000,000 for the PRFM and 1 : 400,000 for the SRFM for all epochs. Table 2 summarizes the results of the computations after con-

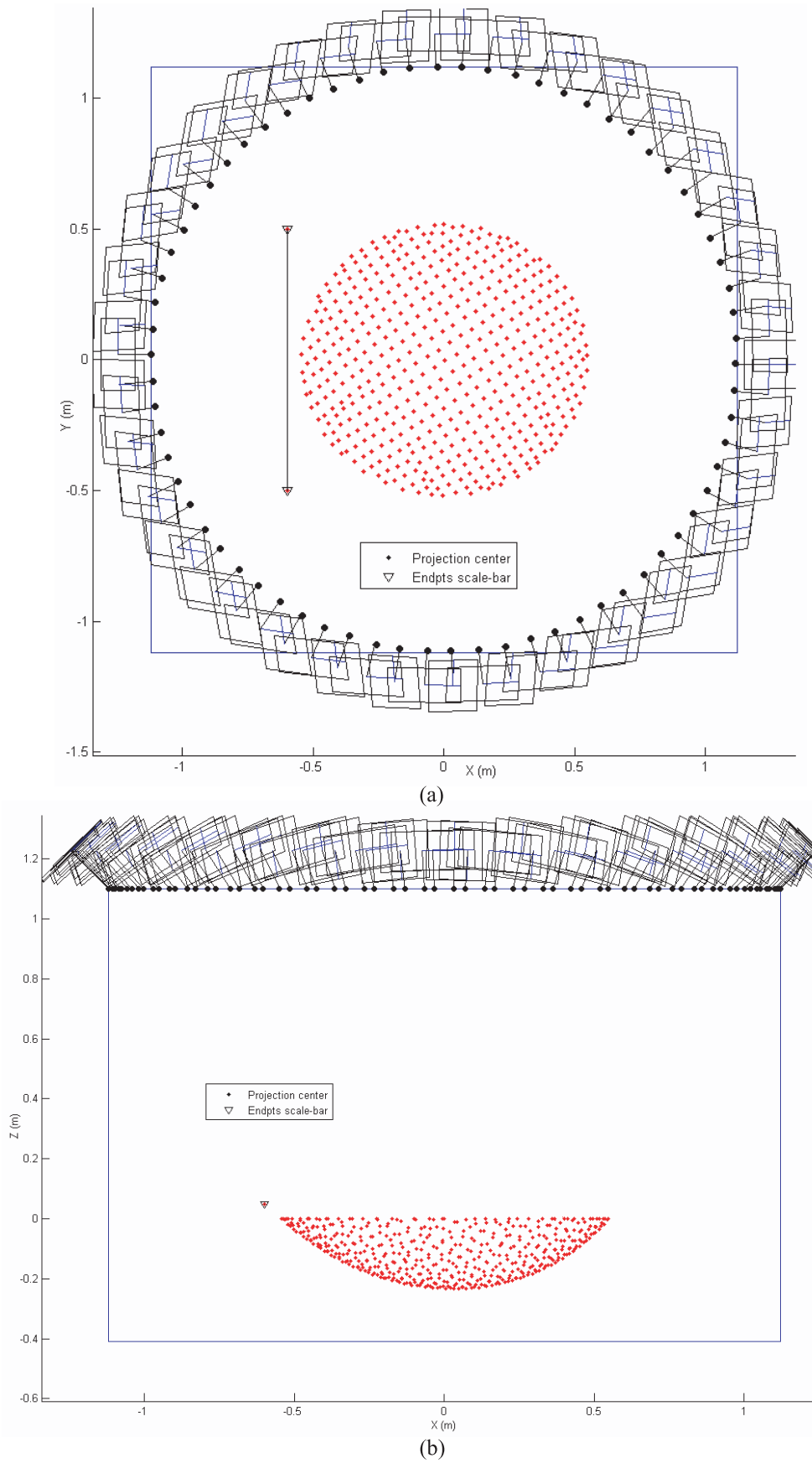

Figure 4: Network configuration for the SR. (a) XY-view and scale-bar, (b) XZ-view of the network.

Table 2: Results of the PRFM and SRFM measurements at ambient temperature and pressure. Precisions are related to one-sigma.

	PRFM	SRFM
Number of images	*65*	*67*
Average number of points in each image	*2200*	*800*
Average number of rays of each point	*62*	*45*
RMSE of the image point residuals (pixel)	*0.011 (1/90)*	*0.012 (1/80)*
Maximum semi-axis of the object point error ellipsoids (microns)	*3.2*	*5.0*
Mean std. dev. values along X, Y and Z axes (microns)	*1.7, 1.8, 2.1*	*2.5, 2.6, 3.2*
Mean relative precision[1] *of the object points*	*1 : 1,000,000*	*1 : 400,000*
Global internal reliability	*0.97*	*0.96*
Average condition number[2] *for the object points*	*0.66*	*0.70*
Maximum isotropy[3] *for the object points*	*0.51*	*0.41*

[1] $\textit{Mean relative precision} = \dfrac{\text{mean}(\sigma_X, \sigma_Y, \sigma_Z)}{\textit{diamater of monitoring object}}$

[2] $\textit{Condition number} = \dfrac{\lambda_{\min}}{\lambda_{\max}}$ *with* λ *the semi-axis of the error ellipsoid*

[3] $\textit{Isotropy} = \dfrac{\max(\sigma_X, \sigma_Y, \sigma_Z) - \min(\sigma_X, \sigma_Y, \sigma_Z)}{\text{mean}(\sigma_X, \sigma_Y, \sigma_Z)}$

version from LEP to TEP. It should be noted that precision values are achieved from the covariance matrix of point coordinates. Thus they define the internal precision which only corresponds to accuracy if no systematic model errors, weight errors or blunders are in the system.

This extremely high precision could be achieved by highly redundant image acquisition. An average of 66 images was acquired in each epoch containing 2200 targets with an average number of 62 rays per point for the PRFM and 800 targets with an average of 45 rays per point for the SRFM.

Blunder detection was done automatically using a dynamic threshold based on RMS values of image point residuals.

Through the analysis of the target center eccentricity in image space, a 6 mm target size was selected. To decrease systematic errors caused by the eccentricity of the target center in object space, the rays with incidence angle greater than the criterion which was computed in the design step, were not used in the computations.

The influence of the target un-flatness was already reduced in the previous step of design while a minimal acceptable target size was selected to reduce the target center eccentricity. Due to the different surface curvature within each reflector, this systematic error is not constant and also differs for each reflector. The maximum systematic error of target un-flatness is estimated to be 7 and 3 microns for SRFM and PRFM, respectively. This error shows its influence mainly on the radius of curvature.

To compensate for systematic errors of the camera, Brown's additional parameters set (Brown 1976) with 8 Additional Parameters (APs) and 2 APs for correction of affinity and shear of the CCD-chip coordinate axes were applied. Figure 5 shows the image space pattern of the systematic errors which was modeled by APs. The maximal size of the residuals is in the order of 80 pixels.

The significance tests of parameters were done with both one-dimensional and multi-dimensional tests. All APs are significant and no correlations higher than 0.9 were found between APs except for the 3 radial symmetrical lens distortions parameters. No correlation higher than 0.85 is present between APs and object point coordinates and between APs and exterior orientation parameters of the camera. Therefore, the estimation of the object point coordinates is highly reliable, taking into account the redundancy of the observations.

The optical parameters were estimated by the developed best-fit ellipsoid method and by choosing an appropriate datum. Since all targets are of the same type (with the same thickness) the best-fit ellipsoid was computed in a first step to estimate the parameters of the ellipsoid. These parameters were used for the determination of the normal vectors to the surface of the reflectors. The measured thickness of the targets and its standard deviation, were used to correct for the thickness of the target. The standard deviations of the target thickness and the point coordinates were used to estimate precision values of the point coordinates by error propagation. After that, the ellipsoid fitting was performed for the SRFM and PRFM and optical parameters were estimated. Large residuals because of the target displacements were eliminated from the computations in the case of PRFM.

4. Conclusions

For the deformation monitoring of the Planck Telescope Reflectors three steps of network design: SOD, FOD and ZOD were executed in order to optimize and simplify the whole design procedure. In SOD the precision of the target center coordinates was estimated from the requested precision of the optical parameters of the PR and SR. A best-fit ellipsoid through least squares surface modeling was developed based on the given model of the reflector to relate the point coordinates to the optical parameters. FOD was performed by heuristic simulation to find

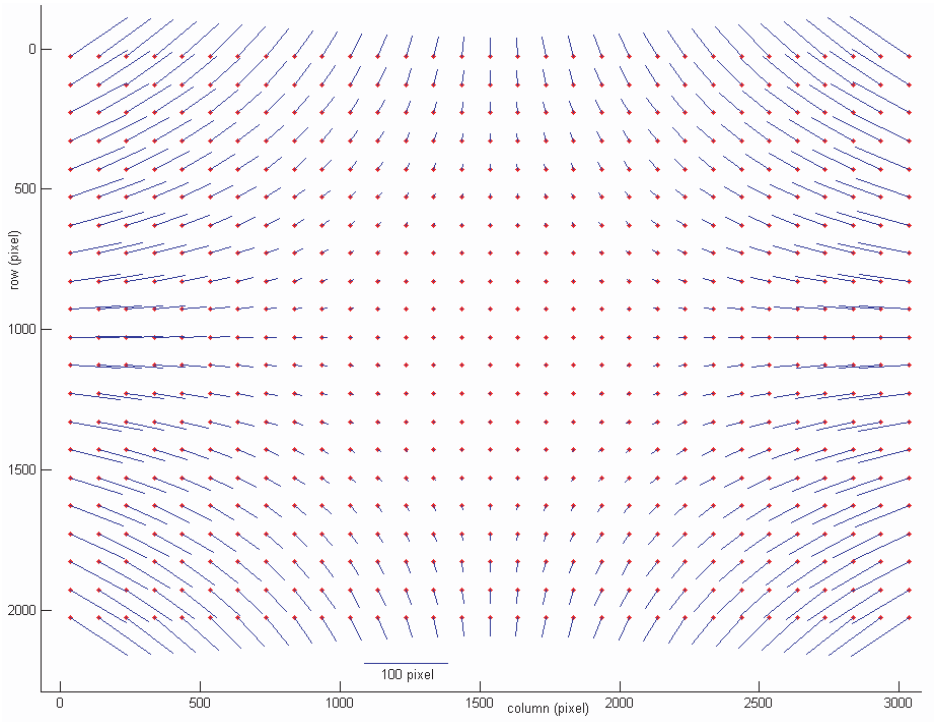

Figure 5: Image space pattern of the systematic errors of the camera.

an optimal configuration of camera stations in order to self-calibrate the system, reduce the influence of the target center shift in the image space, reduce the variation of the target reflectivity of the retro-reflective targets and achieve the estimated precision of the point coordinates in the previous design step (SOD). ZOD was performed in order to achieve the best possible precision of the optical parameters. Through this procedure an optimal close-range photogrammetric network was designed by heuristic simulation with a mean relative precision better than 1:1,000,000 for the PR and better than 1:400,000 for the SR.

Real measurements of the PRFM and the SRFM were performed based on the designed networks by Thales Alenia Space France under ESA-ESTEC contract at 11 epochs with a lowest temperature at 95K using a 6-MegaPixel commercial frame array CCD camera. The RMS errors of the image point residuals were better than 1/70 pixel in measurement of the PRFM and the SRFM. The mean object point standard deviations of the measured 3D points were 1.8 and 2.1 microns for the lateral and depth axes in the case of the PRFM and 2.6 and 3.2 microns for the lateral and depth axes in the case of the SRFM. This extremely high precision could be achieved by a strong geometrical network, the concept of hyper-redundancy, efficient blunder detection methods, advanced network design for self-calibration and taking into consideration the influence of the target center eccentricities.

The validation of the results is carried out with other independent accurate techniques: Coordinate Measurement Machine (CMM) and Interferometery. The initial assessment shows the consistency of the photogrammetric measurement results with respect to the results from two the other techniques. A quantitative method for the assessment of the results is in progress.

Disclaimer

This article has been prepared for information purposes only. It is not designed to constitute definitive advice on the topics covered and any reliance placed on the contents of this article is at the sole risk of the reader.

Acknowledgements

The Planck project was funded by European Space Agency. The authors thank Philippe Kletzkine, the manager of the Planck Telescope Reflectors test, who supported this project. We also appreciate Thales Alenia Space France for the execution of the test.

References

Amiri Parian, J., Close-range Photogrammetric Network Design Based on Micro-Cameras for Herschel Spacecraft, Technical report for ESA-ESTEC, 2004.

Amiri Parian, J., Gruen, A. and Cozzani, A., High Accuracy Deformation Monitoring of Space Structures by Heuristic Simulations, Third IAG Symposium on Geodesy for Geotechnical and Structural Engineering and 12th FIG Symposium on Deformation Measurements, 2006.

Brown, D. C., The Bundle Adjustment – Progress and Prospects. In: International Archive of Photogrammetry, Helsinki, Finland, Vol. 21, Part B3, 1976.

European Space Technology and Research Centre, http://www.esa.int/esaCP/SEMOMQ374OD_index_0.html (Last date accessed: June 2007).

Fraser, C. S., Network Design Considerations for Non-Topographic Photogrammetry, Photogrammetric Engineering and Remote Sensing, 50 (1984), 1115–1126.

Fraser, C. S., Limiting Error Propagation in Network Design, Photogrammetric Engineering and Remote Sensing, 53 (1987), 487–493.

Fraser, C. S., Photogrammetric Measurement to One Part in a Million, Photogrammetric Engineering and Remote Sensing, 58 (1992), 305–310.

Fraser, C. S., Network Design, Chapter 9. Close Range Photogrammetry and Machine Vision (Ed. Atkinson, K. B.), Whittles Publishing, Scotland, 1996.

Fraser, C. S., Woods, A., Brizzi, D., Hyper Redundancy for Accuracy Enhancement in Automated Close-range Photogrammetry, The Photogrammetric Record, 20 (2005), 205–217.

Fritsch, D. and Crosilla, F., First Order Design Strategies for Industrial Photogrammetry, SPIE Vol. 1395, Close-Range Photogrammetry Meets Machine Vision, 1990, 432–438.

Grafarend, E., Optimization of Geodetic Networks, Bollentino di Geodesia a Acience Affini, 33 (1974), 351–406.

Gruen, A., Accuracy, Reliability and Statistics in Close-Range Photogrammetry, Symposium of ISP, Commission V, Stockholm, 1978.

Gruen, A., Precision and Reliability Aspects in Close-Range Photogrammetry, XIV Congress of ISP, Commission V, Hamburg, 1980.

Gruen, A. and Beyer, H., System Calibration Through Self-Calibration, in: Calibration and Orientation of Cameras in Computer Vision (Eds. Gruen, A. and Huang, T. S.), Springer-Verlag, Berlin Heidelberg, 2001.

Mason, S., Expert System-Based Design of Photogrammetric Networks, Institute of Geodesy and Photogrammetry, ETH Zurich, Switzerland, PhD Thesis, 1994.

Olague, G., Automated Photogrammetric Network Design Using Genetic Algorithms, Photogrammetric Engineering and Remote Sensing, 68 (2002), 423–431.

Passvogel, T., Juillet, J.-J., The Current Status of the Herschel/Planck Programme, Proceedings of SPIE, Vol. 4850, 2003, 598–605.

Saadatseresht, M., Fraser, C. S., Samadzadegan, F. and Azizi, A., Visibility Analysis in Vision Metrology Network Design, The Photogrammetric Record, 19 (2004), 219–236.

Tauber, J. A., The Planck Mission: Overview and Current Status, Astrophysics Letters & Communications, Vol. 37, 2000.

Thales Alenia Space, http://www.thalesonline.com/space (Last date accessed: June 2007).

Torlegard, K., On Accuracy Improvement in Close-range Photogrammetry, Proceedings of Industrial and Engineering Survey Conference, London, 1980.

Wimmer, H., Second Order Design of geodetic networks by an iterative approximation of a given criterion matrix, in: Deutsche Geodätische Kommission, Reihe B, Heft 258/III, 1982, 112–27.

Received: Dec 12, 2006 Accepted: Mar 1, 2007

Author information

Jafar Amiri Parian, Armin Gruen

Institute of Geodesy and Photogrammetry, ETH Zurich, Switzerland

E-mail: (amiriparian, agruen)@geod.baug.ethz.ch

Alessandro Cozzani

European Space Agency – ESTEC (TEC-TCE), the Netherlands

E-mail: alessandro.cozzani@esa.int